10

Manipulation of Nanorods on Elastic Substrate, Modeling and Analysis

A. H. Fereidoon[1], M. Moradi[1] and S. Sadeghzadeh[2,*]
[1]*Department of Mechanical Engineering, Semnan University, Semnan,*
[2]*Department of Mechanical Engineering,*
Iran University of Science and technology (IUST), Tehran,
Iran

1. Introduction

Nanorods are one of the nano-scale structures in nanotechnology that may be synthesized of metal or semiconductor materials. Nanorod range of applications is different, ranging from display technology (reflection of the nanorod can be changed by applying electric field) to build Micro Electro Mechanical systems (MEMS).

Nano-manipulation, or controlled positioning at nanoscale, is the first step towards fabrication and assembly purposes. In this process, the Atomic Force Microscope (AFM) tip makes contact with nanoparticles and pushes them on the substrate. The AFM deflections during pushing task can be sensed and recorded using photodiode and optical methods.

This chapter of the book reviews manipulation of nanorods in various functional conditions. This review includes:

- Nanorod applications
- Different types of nanorods
- Applications of nanorods kinesiology in different technology
- Different methods of manipulation of Nanorods.
- Classification of effective parameters in manipulation of Nanorods
- Effective forces and available theory in nanorod modeling
- Various theories to model nanorod
- Appropriate strategy for manipulation of Nanorods and efficient algorithm
- A complete sample modeling and motion simulation
- The basic variables and their effects in manipulation

1.1 Nanorod applications, applications of nanorods kinesiology in different technology

The applications of nanorods are diverse, ranging from display technologies (the reflectivity of the rods can be changed by changing their orientation with an applied electric field) to

*Corresponding Author

MEMS. Nanorods based on semiconducting materials have also been investigated for application as energy harvesting and light emitting devices (wikipedia website).

Prominent among them is in the use in display technologies. By changing the orientation of the nanorods with respect to an applied electric field, the reflectivity of the rods can be altered, resulting in superior displays. Picture quality can be improved radically. Each picture element, known as pixel, is composed of a sharp-tipped device of the scale of a few nano meters. Such TVs, known as field emission TVs, are brighter as the pixels can glow better in every colour they take up as they pass through a small potential gap at high currents, emitting electrons at the same time.

Nanorod-based flexible, thin-film computers can revolutionize the retail industry, enabling customers to checkout easily without the hassles of having to pay cash (articleworld website).

1.2 Different types of nanorod

There are several demands to use manipulation of Nanorods based on how the nanowire is placed on the sample substrate (fig 1a-c). Also, different kinds of nanorod such as biological, metallic, etc exist in nature and industry. Rigid particles can be moved without considerable deflection; flexible particles can be moved with considerable deflection; but soft particles may be damaged when pushing force exceeds the yield stress (Fig. 1).

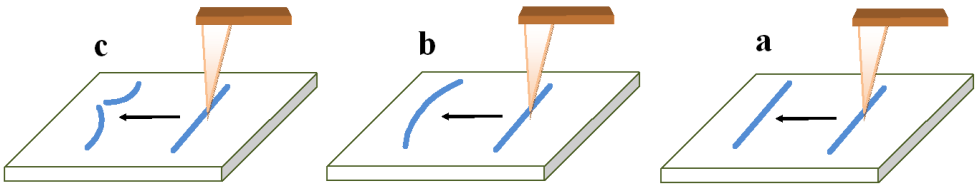

Fig. 1. Three expected results: a- rigid nanorod, b- flexible nanorod, c- soft nanorod

1.3 Different methods of manipulation of nanorods

Generally, there are two methods for nanorod and nanowire manilulation. These are Pick/Place and Push/Pull. Figures 2 and 3 show strategies for Pick/Place and Push/Pull manipulation, respectively.

2. Manipulation of nanorods

2.1 Classification of effective parameters on manipulation of nanorods

In the AFM, there are five effective parts in manipulation and each of them has different parameters (Table1). Several processes can be designed composing these parts and their parameters.

2.2 Effective forces in manipulation of nanorods

There exist various nano forces in the AFM based nano-manipulation with a micro probe. However, what are main forces and how they work to remain not very clear (Tian et al.,

2007). Based on the recent researches (Bhushan, 2005; Israelachvili, 1991) and considering effective factors such as humidity and electrostatic charge, the crucial nano forces can be summarized as van der Waals, repulsive contact force and friction (three basic nano forces). Furthermore, the capillary force aroused by humidity or biological substrates, where, the electrostatic force caused by the electrostatic charge. Based on their effect in nano-manipulation, these forces can be categorized into attractive, repulsive and frictional forces (Tian et al., 2007) . The nano forces between tip and particle can be described as shown in figure 4.

General Factors	1	2	3	4
Manipulation Task	Push/pull	Pick/Place	Cutting	Bending/ Buckling
AFM Specification	Contact/Non-contact/ Tapping Mode	Wet/Dry Environment	Cantilever/ Gripper	Rectangular/ V Shaped Cantilever
Particle	Sphere/Rod/Tube	Dimensions	Rigid/Elastic	Metallic/ Biologic
Substrate	Smooth/Rough	Rigid/Elastic	Metallic/ Biologic	Solid/ Fluid
Process Dynamics	Dominant Forces	2D/3D	Straight/Curved Path	Constant Velocity/Acceleration

Table 1. General effective parts and parameters in manipulation process (Moradi et al., 2011)

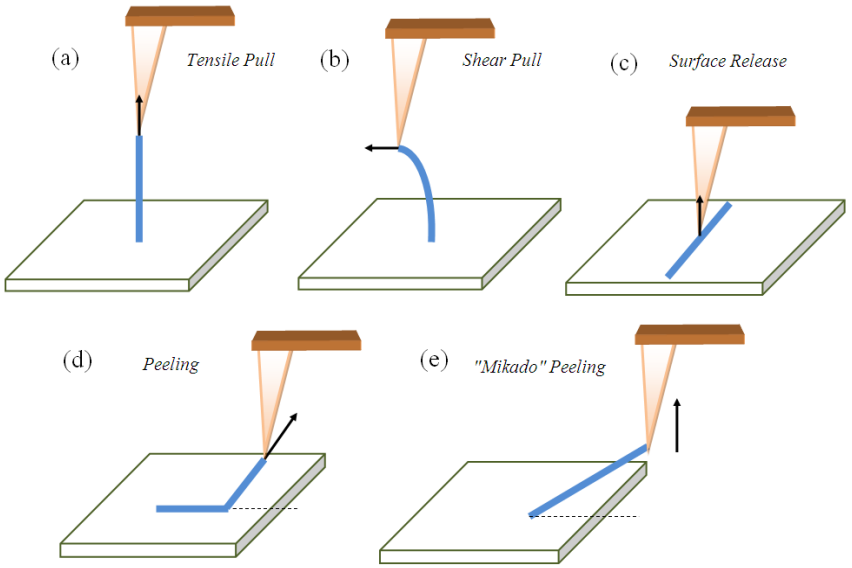

Fig. 2. Strategies for picking up a nanorod. Picking nanorods can be done by pulling along (a) or sideways (b) to the axis of a standing nanorod. Nanorods lying on substrates can beare attractiv ich consistforces,tractive van der Waals force, capillar are repulsive forces composed of repulsive contact force, repulsive van der Waals force and repulsive electrostatic force, respectively (Sitti & Hashimoto, 2000).

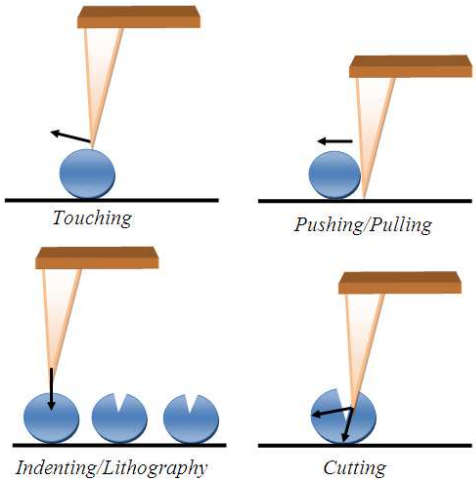

Fig. 3. Possible mechanical push/pull task using AFM probe

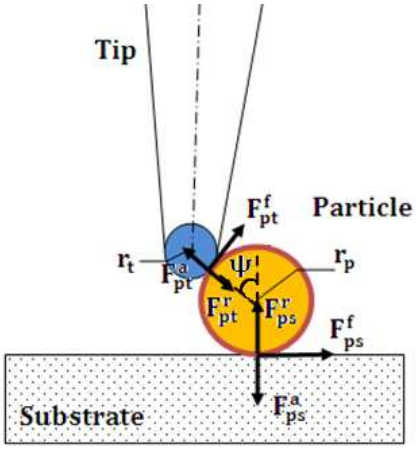

Fig. 4. The nano forces among tip, particle and substrate (Sitti & Hashimoto, 2000)

Where subscripts *p, t* and *s* correspond to probe, tip and substrate and superscripts *f, r* and *a* correspond to the friction, repulsive and attractive forces, respectively. F_{ts}^{f} and F_{pt}^{f} are rictional forces, F_{ps}^{a} and F_{pt}^{a} are attractiv ich consistforces,tractive van der Waals force, capillary force and attractive electrostatic force, and F_{ps}^{r} and F_{pt}^{r} are repulsive forces composed of repulsive contact force, repulsive van der Waals force and repulsive electrostatic force, respectively (Sitti & Hashimoto, 2000).

Like gravitational force, van der Waals forces exist for every material in any ambient condition. These forces originate from electromagnetic forces between two dipoles and depend on material types, separation distances and object geometry (Bhushan, 2005) . For spherical tip-flat surface, the van der Waals force is as

$$f(h)_{wdv} = -\frac{A_H R_t}{6h^2} \quad (1)$$

Where A_H, R_t and h are Hamaker constant (about 10^{-19}), tip radius and distance between tip and substrate, respectively. The minus sign indicates attractive force and the plus sign indicates repulsive one (Serafin & Gewirth, 1997). When the tip approaches to the substrate, reaches to a region of mechanical instability that the force gradient of the potential F_{pt}^{f} exceeds the spring constant of the cantilever (Serafin & Gewirth, 1997)

$$\frac{df(h)_{wdv}}{dh} = K_Z \quad (2)$$

At this instability, the probe will jump into contact with the surface with a characteristic "snap-in" distance, d_s as

$$d_s = \left(\frac{A_H R_t}{3K_Z}\right)^{1/3} \quad (3)$$

Snap in substrate phenomena using photodiode data can be detected (Serafin & Gewirth, 1997).

The water layers on the surfaces of probe, particle, or substrate result in the adhesion force. A liquid bridge occurs between the tip surfaces at close contact (Sitti & Hashimoto, 2000). The adhesion force between a non-deformable spherical particle of radius R_t and a flat surface in an atmosphere containing a condensable vapor is

$$F_S = 4\pi R_t(\gamma_{LV}\cos\varepsilon + \gamma_{SL}) \quad 4)$$

Where ε is the contact angle, the first term is due to the Laplace pressure of the meniscus (γ_{LV} : Liquid-Vapor surface energy) and the second one is due to t: Solid-Liquid surface energy) (Israelachvili, 1991).

As there will be some electrical charge accumulated on the surface of particles or the tip, the particle is prone to adhere on the tip and manipulation may be failed. Since the particles are not picked up, the electrostatic force between the particle and the substrate is not important. However, after pushing, the charge on the particle is transferred to the tip which can cause an electrostatic force. Electrostatic force between tip and substrate will be as

$$F_e = \kappa R_t Z e^{\kappa h} \quad (5)$$

Where is the Debye length, Z is the characteristic parameter of the tip - particle and h is distance (Bhushan, 2005) . In actual experiment condition, probe and substrate can be grounded to release the electrostatic charge for minimizing electrostatic force and also the experiment condition can be kept dry to minimize the capillary force. Thus, the crucial forces between the tip and the substrate are mainly van der Waals, Friction and repulsive contact force (Tian et al., 2007) .

Contact force causes the indention on contact surfaces, which is considerable in nano-scale and affect the manipulation. Several models like Hertz, Johnson–Kendall–Roberts (JKR),

Maugis–Dugdale (MD) has been utilized as the continuum mechanic's approaches in nanoscale (Bhushan, 2005) . The Hertz model only takes consideration of mechanical deformation under external force. However, the surface adhesion force becomes significant in the contact of micro and nano objects, which must be taken into consideration. Using JKR model (Bhushan, 2005) , the adhesion force (F_{adh}) and the surface energy (W_{adh}) are related as

$$F_{adh} = -\frac{3}{2}\pi R_t W_{adh} \tag{6}$$

In JKR theory, the contact radius was found to be

$$a^3 = \frac{R}{K}(P_0 + 3\pi RW + \sqrt{6\pi RWP_0 + (3\pi RW)^2} \tag{7}$$

Where P_0, R, a and K are normal force, equivalent radius, contact radius and equivalent elastic modulus of particle- surface, respectively (Israelachvili, 1991). R and K are as

$$K = \frac{4}{3}[\frac{1-\nu_1^2}{E_1} + \frac{1-\nu_2^2}{E_2}]^{-1} \tag{8}$$

$$R = \frac{R_1 R_2}{R_1 + R_2} \tag{9}$$

Where ν_i and E_i are poisson ratio And modulus of elasticity in (8). R_1 and R_2 are radius of curvature of particle and surface in (9), respectively. Contact area has an important effect in nanorod friction and so in motion behavior. Friction in nanoscale can be calculated as

$$f = \mu F + S_c A \tag{10}$$

Where μ, F, S_c and A are friction coefficient, normal force, critical shear stress and contact area (Bhushan, 2005) .

3. Theories for nanorod modeling

Common approaches to model cylindrical elastic system are Euler-Bernoulli and Timoshenko beam theory (Falvo et al., 1999; Falvo et al., 1997; Wu et al., 2010; Hsu et al., 2008). Falvo et al. studied behavior of a TMV virus using Euler- Bernoulli beam. In another work, they modeled CNTs as an Euler- Bernoulli beam to study rolling and sliding in nanoscale. Also, Hsu et al. used Timoshenko beam theory on the elastic substrate to calculate natural frequencies and mode shapes of CNTs (Hsu et al., 2008). Wu et al. manipulated CNTs with various diameters using a cantilever tip of the AFM to investigate the motion properties. They used Euler- Bernoulli theory to model flexible behavior of one-dimensional nanomaterials on a structured surface (Wu et al., 2010). In the present study, at the first time, manipulation process is considered nanorod as an Euler- Bernoulli beam on the elastic substrate (Fig. 5).

Euler- Bernoulli equation is as

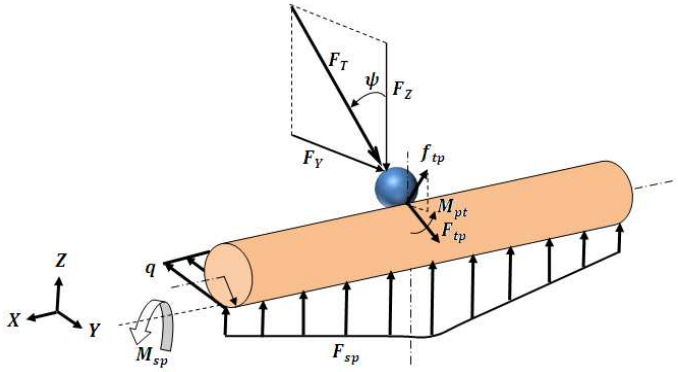

Fig. 5. Free-body-diagram of nanorod and corresponding parameters

$$EI\frac{\partial^4 y}{\partial x^4} = -K_s y \tag{11}$$

Where y, K_s, E and I are deflection in a plane perpendicular to the substrate, elastic constant of substrate- nanorod interface, nanorod modulus of elasticity and moment of inertia. General solution of equation is

$$y = e^{-\beta x}\left(C_1\cos\beta x + C_2\sin\beta x\right) + e^{\beta x}\left(C_3\cos\beta x + C_4\sin\beta x\right), \beta = \sqrt[4]{\frac{K_s}{4EI}} \tag{12}$$

Due to fourth order equation, we need four boundary conditions (Boresi et al., 1993). These boundary conditions can be defined as pushing force in center of nanorod and finiteness of nanorod length. So, boundary conditions in finite beam are

$$\begin{cases} x \to \pm\dfrac{L}{2} \Rightarrow M = EI\dfrac{d^2y}{dx^2} = 0 \\ x = 0 \Rightarrow \Theta = \dfrac{dy}{dx} = 0 \\ x \to 0^+ \Rightarrow V = -EI\dfrac{d^3y}{dx^3} = -\dfrac{P}{2} \end{cases} \tag{13}$$

Where Θ, P, V and M are deflection angle, normal pushing force, shear force and moment. Using definition $a = \dfrac{P}{8EI\beta^3}$, exact solution will be (Boresi et al., 1993)

$$y = \frac{2ae^{\beta(L-x)}}{1-e^{2\beta L}}\left[-\left(1+e^{\beta L}\right)\cos\beta x + (1-e^{\beta L})\sin\beta x\right] + \frac{2ae^{\beta x}}{1-e^{2\beta L}}\left[-\left(1+e^{\beta L}\right)\cos\beta x + (1-e^{\beta L})\sin\beta x\right] \tag{14}$$

Mechanical model of an elastic nanorod under pushing force is illustrated in figure 6, schematically. In this figure, A and B are the ends of the sample; T is the push point. Unlike prior works, q changes along the nanorod length as friction force. Which q in each section can be obtained as

$$q(x)=\frac{\mu F}{L}+\frac{S_c A(x)}{L} \tag{15}$$

Where μ, S_c , L and A are friction coefficient, critical shear stress, length of nanorod and contact area. In each instance, contact area using JKR model calculates and adds to (15). According to contact area along the length, this relation improves accuracy of the model. So, deflection deviation along length can be obtained as (Boresi et al., 1993)

$$\begin{cases} U=-\dfrac{q(x)x^2}{24EI}\left(4Lx+x^2+6L^2\right), -\dfrac{L}{2}<x<0 \\ U=+\dfrac{q(x)x^2}{24EI}\left(4Lx-x^2-6L^2\right), 0<x<\dfrac{L}{2} \end{cases} \tag{16}$$

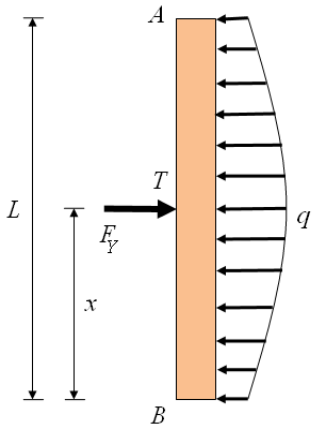

Fig. 6. Free-body-diagram of nanorod along path

In this problem, both the substrate and the nanorod are stationary at the beginning. Then, the probe moves with constant velocity and pushing force causes deflection along the path.

4. Strategy and algorithm for manipulation of Nanorods

The manipulation process cannot be observed in real time. During the pushing of the objects, imaging is not possible because imaging and manipulation tools are same. As a solution, surface and targeted particles could be imaged before and after manipulation. Using the obtained images, relative position of particles to the basic reference point can be determined (Requicha, 1999). Due to lack of real time images using the force feedback data during the for proper manipulation is crucial.

Two methods can be considered for pushing nanoparticles in constant speed: (1) Moving the substrate while AFM probe is in contact with particle; (2) AFM probe tip moves and pushes the targeted particle on the immobile substrate. Dynamic results for both methods would be the same (Korayem & Zakeri, 2008; Tafazzoli et al., 2005). The first method is used in this paper where the probe forces F_T acting between the tip and the particle is kept constant during nanoparticles movement on substrate (Fig. 7).

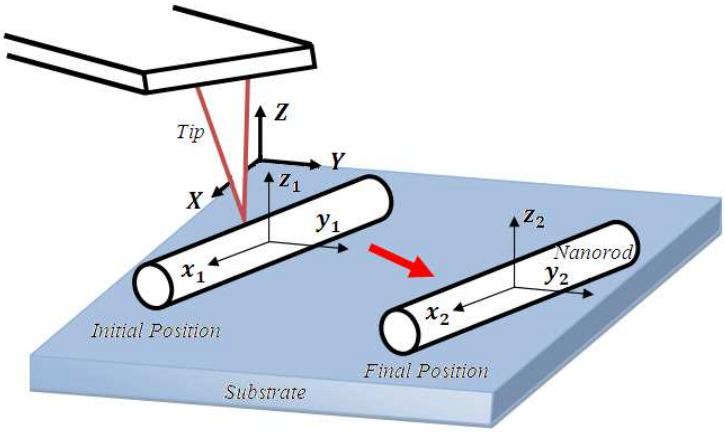

Fig. 7. AFM tip moves nanorod on substrate (Moradi et al., 2010)

4.1 Manipulation strategy

As mentioned above, at the beginning of the process both the substrate and particle are in the stationary state. Then, the probe moves down to approach substrate (Auto Parking). Van der Waals force increases until snap in instability point, respectively. In this point, the tip jumps to the substrate. This phenomenon can be detected using photodiode data. Then the tip starts to move upward. Deflection in the cantilever increases until pulling force overcame attraction force. According to the adhesion force between the tip and substrate, retraction force is more than attraction force. Next, the tip moves to reach the desired particle, horizontally. Also, van der Waals force between the tip and the particle increases until snap in particle. Then, the substrate motion follows and pushing force on particle increases. The tip may be crossed the particle and the process being failed. To ensure the desired contact, a small normal preload, F_{z0} is exerting by providing normal deflection offset, Z_{P0} on the AFM probe. Then, substrate moves in constant velocity and particle sticks to that and moves with substrate. Lateral motion of particle assists to increase pushing force, *FT*. Finally, pushing force reaches to the critical force required to overcome adhesion forces between particle/substrate. The particle motion with the substrate stops, when particle reached to desired position. At this time, the suggested behavior will be expected by particle depending on dynamic mode diagrams of particle. The probe moves upward and goes to the initial reference position when process completes (Fig. 8).

4.2 Manipulation algorithm

A new algorithm is presented to manipulate nanorods automatically (Fig. 9). As mentioned in manipulation strategy, both actuator and sensor in the AFM as nanorobots are same. Due to the image- manipulation- image cycle of the process for proper manipulation this algorithm has three parts; imaging before motion, manipulation and imaging after manipulation (Requicha, 1999).

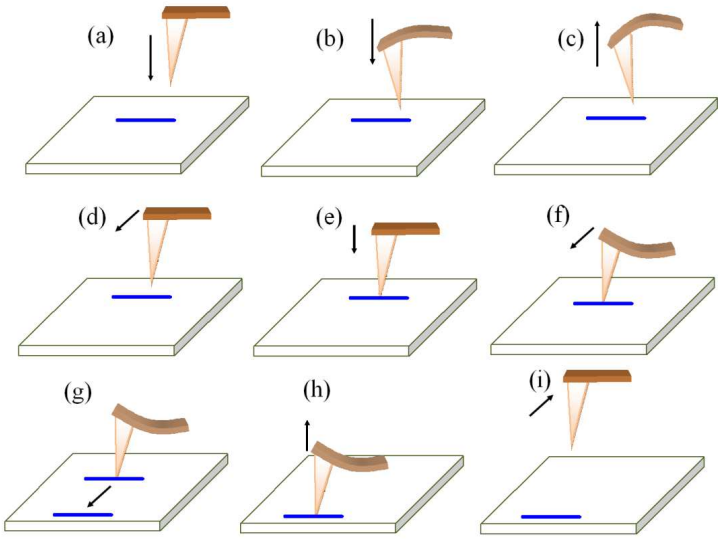

Fig. 8. Nano-manipulation strategy using the AFM: a) Auto parking, b) Snap in substrate, c) Pull out substrate, d) Approach to nanorod, e) Snap in nanorod, f) Offset in Z direction, g) Pushing, h) Pull out nanorod, k) Going to Reference point (Moradi et al., 2011)

In manipulation before motion, the AFM in the non-contact mode starts imaging and specifies particle geometries. User can choose particles and their desired position to the operation. Then the AFM detects center of particles. If the center of particles placed in the desired position, the process will be finish. Otherwise, second part of process will be start. In the second part, after contact between the probe- particle, stage moves with defined constant velocity. This motion makes the cantilever bend and increase pushing force. As mentioned above, pushing force affects on deformation, depression and indention of particle and substrate. According to the presented model these changes can be obtained and damage condition can be checked for different kinds of nanorods. If primary pushing force don't damage nanorod, the pushing should be follow to desired place.

Stage turn down when the particle pushing take place. In third part, the AFM scans the path in line backward and controls achievement. If the particle had been placed in desired position with minimum deviation, the process completed. It may some deviation occur due to different nonlinearities such as drift, creep and hysteresis in the process. When there is deviation, the AFM goes to the second part and process continues until the particle reaches to its destination.

5. Complete modelling

The AFM nanorobot has a cantilever as a manipulator. This cantilever probe consists of a connected canonical tip. The AFM is modelled as a linear spring to account for normal deflection in z direction, and a torsional spring to record lateral twisting of the probe. Spring coefficients of the springs in expression (17) (Tafazzoli et al., 2005) are a function of the geometry and the mechanical properties of the AFM probe.

$$K_z = \frac{Ewt^3}{4L^3}, K_\theta = \frac{Ewt^3}{6L(1+\upsilon)} \tag{17}$$

Where L, w, and t are the length, width, and thickness of the cantilever. E and ν are the young's modulus and poison's ratio of the probe, respectively.

Spring force/moment is linear product of the spring constant and deflection/twisting. Spring force and moment (F_z, M_θ), shear force (F_v), normal (F_Z) and lateral tip force (F_Y), and tip pushing force (F_T) are depicted during lateral movement of the particle in AFM tip free body diagram (Fig. 10).

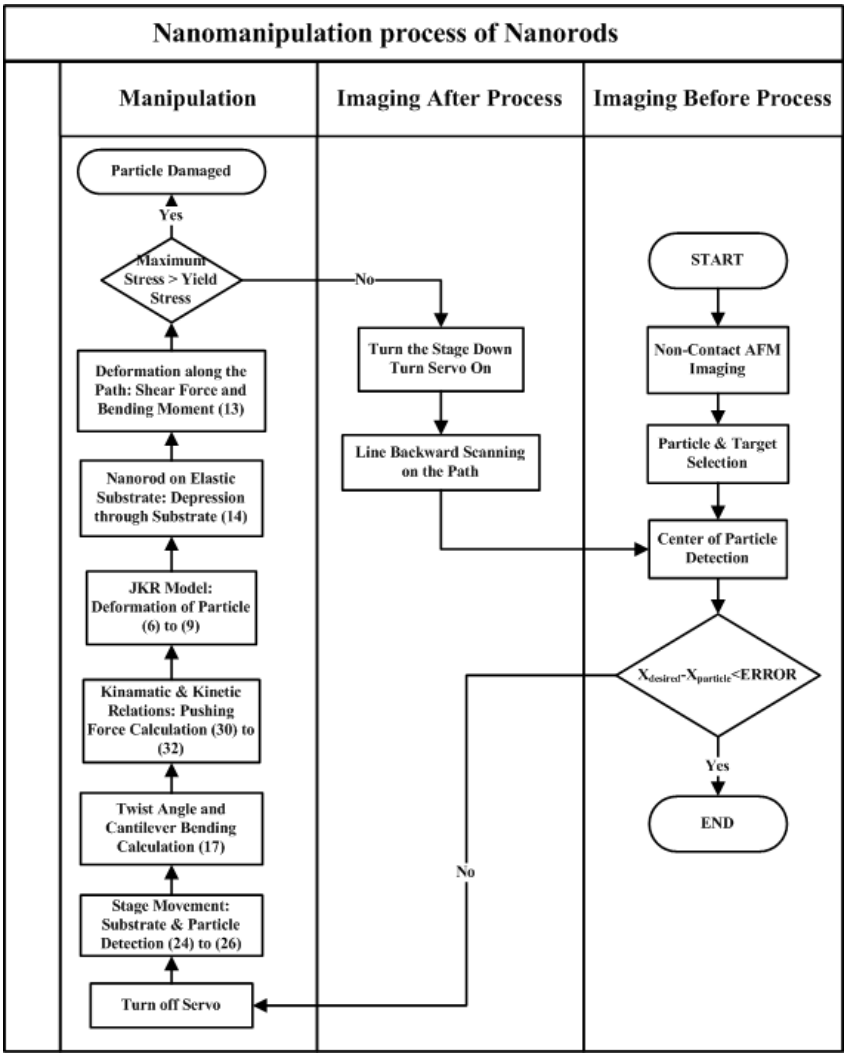

Fig. 9. Manipulation of Nanorods algorithm

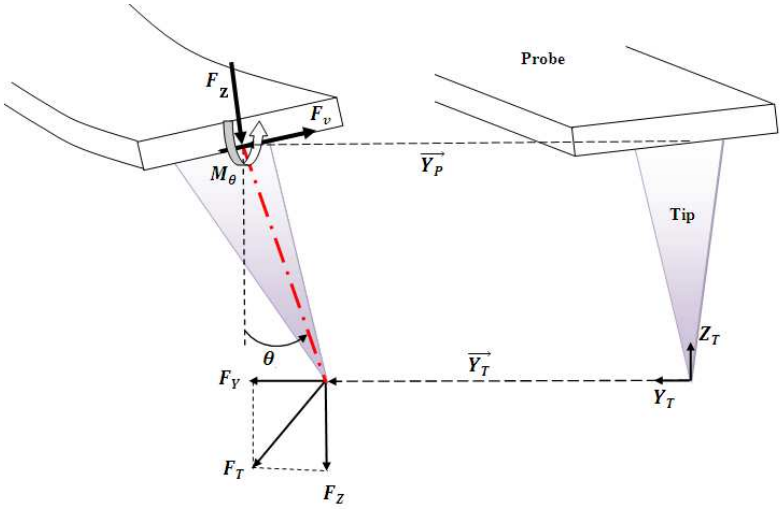

Fig. 10. Free body diagram of the AFM tip and corresponding parameters

Since the nano-manipulation task is implemented by the very front part of the tip which is very small compared with the whole probe tip body, the forces applied on tip can be viewed as applied on the tip apex (Sitti & Hashimoto, 2000).

Van der Waals force between the cantilever tip and the flat surface is as

$$f_1(h) = -\frac{A_H R_t}{6h^2} \tag{18}$$

Where A_H, R_t and h are Hamaker constant (about 10^{-19}), tip radius and distance between tip and substrate, respectively. The minus sign indicates attractive force and the plus sign indicates repulsive one (Dong & Mao, 2005). When tip approaches to substrate, reaches to a region of mechanical instability that the force gradient of the potential exceeds the spring constant of the cantilever (Dong & Mao, 2005)

$$\frac{df(h)_{wdv}}{dh} = K_Z \tag{19}$$

At this instability, the probe will jump into contact with the surface with a characteristic "snap-in" distance, d_s as

$$d_s = \left(\frac{A_H R_t}{3K_Z}\right)^{1/3} \tag{20}$$

Snap in substrate phenomena using photodiode data can be detected (Dong & Mao, 2005). Then the probe moves upward until spring force equals to pull out force (21).

$$f_2(h) = -\frac{3}{2}\pi R_t W_{adh} = -K_Z Z_P \tag{21}$$

Now, the probe approaches to the nanorod, horizontally. Van der Waals force between the tip and the nanorod increases when the distance decreases (Serafin & Gewirth, 1997). This force and snap in point are presented in (22) and (23).

$$f_3(h) = -\frac{A_H R_{pt}^{1/2}}{8\sqrt{2}h^{5/2}}, R_{pt} = \frac{R_p R_t}{R_p + R_t} \tag{22}$$

$$d_s = \left(\frac{5A_H R_{pt}^{1/2}}{16\sqrt{2}\mathrm{H}K_\theta}\right)^{\frac{2}{7}} \tag{23}$$

Where H is the tip height. To ensure the contact with the particle a small normal deflection offset is exerted on the AFM probe. The positioning stage is moved with a constant velocity. Assuming this velocity to be small, the quasi-static assumption can be considered to be valid ($\frac{dy_T^2}{dt^2} = 0$) (Korayem & Zakeri, 2008; Tafazzoli et al., 2005). Thus, the lateral position, velocity and acceleration of the tip in Y direction can be defined as relations (24) to (26).

$$\mathrm{y_T} = \mathrm{y_P} - \mathrm{H}\sin\theta \tag{24}$$

$$\dot{y}_\mathrm{T} = \dot{y}_\mathrm{P} - \mathrm{H}\dot{\theta}\cos\theta \tag{25}$$

$$\ddot{y}_\mathrm{T} = 0 - \mathrm{H}\ddot{\theta}\cos\theta + \mathrm{H}\dot{\theta}^2\sin\theta \Rightarrow \ddot{\theta} = \dot{\theta}^2\tan\theta \tag{26}$$

Where P corresponds to the probe and T corresponds to the tip; θ represents the twisting angle of the probe. To determine the dynamics of the system, the normal deflection of the probe (Z_P) is critical.

$$\mathrm{Z_P} = \mathrm{Z_T} - \mathrm{H}\cos\theta; \mathrm{Z_T} = \mathrm{Z_{P0}} + \mathrm{H} = \mathrm{cte.} \tag{27}$$

$$\dot{Z}_\mathrm{P} = \mathrm{H}\dot{\theta}\sin\theta \tag{28}$$

$$\ddot{Z}_\mathrm{P} = \mathrm{H}\ddot{\theta}\sin\theta + \mathrm{H}\dot{\theta}^2\cos\theta \tag{29}$$

Using Newton-Euler method, forces on the AFM tip can be derived as

$$\mathrm{F_Z} = \left(\frac{\mathrm{I_P}\ddot{\theta} - \mathrm{M_\theta}}{\mathrm{H}}\right)\sin\theta + (\mathrm{F_z} - \frac{\mathrm{m}}{2}\ddot{z}_\mathrm{p})\cos^2\theta \tag{30}$$

$$\mathrm{F_v} = \frac{1}{\sin\theta}\left(\mathrm{F_Z} - \mathrm{F_z} + \frac{\mathrm{m}}{2}\ddot{\mathrm{Z}}_\mathrm{P}\right) \tag{31}$$

$$\mathrm{F_Y} = \mathrm{F_v}\cos\theta \tag{32}$$

Where I_p is the AFM tip moment of inertia through its rigid contact with the probe, and m is the mass of the AFM tip. Forces expressions (30) to (32) would determine the pushing force and pushing angle of the nanoparticle.

$$F_T = \sqrt{F_Y^2 + F_Z^2}, \quad \psi = \tan^{-1}(F_Y / F_Z) \tag{33}$$

Where ψ is the pushing force angle. Normal (F) and frictional forces (f) on the particle (Fig. 2) using the pushing force, are derived as (34) to (37)

$$f_t = F_T \cos\zeta, \quad \zeta = \psi - \varphi - \frac{\pi}{2} \tag{34}$$

$$F_t = -F_T \sin\zeta \tag{35}$$

$$f_s = F_T \sin\psi \tag{36}$$

$$F_s = F_T \cos\psi \tag{37}$$

Where t and s corresponds to the AFM tip and the substrate; φ is contact angle. Normal forces (F_t, F_s) would cause deformations on the tip-nanorod and the nanorod- substrate interfaces, respectively.

According to the increase in the lateral pushing force and the contact deformation, frictional force grows and reaches to its critical value. Expressions (38) to (40) indicate sliding and rolling conditions on the tip and the substrate (Tafazzoli et al., 2005).

$$F_s > \mu_{ss} F_s + S_{ss} A_s \tag{38}$$

$$F_t > \mu_{ts} F_t + S_{ts} A_t \tag{39}$$

$$(f_s + f_t) R_p > (M_s + M_t) \quad where \quad M_t = \mu_{tr} F_t + S_{tr} A_t \tag{40}$$

Where s and r correspond sliding and rolling. So, μ_{tr} indicates tip friction coefficient in the rolling mode. Using expressions (34) to (39) and simplifying relations (38) to (40), critical forces for sliding on the tip (41), sliding on the substrate (42) and rolling the nanorod (43) in Y directions are obtained as

$$F^*_{t-Sliding} = \frac{S_{ts} A_t}{\sin\zeta - \mu_{ts} \cos\zeta} \tag{41}$$

$$F^*_{s-Sliding} = \frac{S_{ss} A_s}{\sin\psi - \mu_{ss} \cos\psi} \tag{42}$$

$$F^*_{s-Rolling} = \frac{S_{sr}(A_s + A_t)}{R_p(\sin\psi + \cos\zeta) - \mu_{sr}(\sin\zeta - \cos\psi)} \tag{43}$$

6. Simulations

Aim of this section is simulation of nanorods and studies its behavior during motion. Critical force, critical time, maximum deflection and safety factor are some of the most important

parameters of the process. The Si AFM probe is used to simulate nanorod. Geometrical and mechanical properties of the probe are summarized in Table 2 (Israelachvili, 1991). Due to few available experiments with complete quantitative parameters of materials, the reference 21 is selected for simulation. In this reference, complete parameters for polystyrene particles are presented. Polystyrene is a hard and solid polymer with specified tribological properties (Table 3) (Israelachvili, 1991). Recently, Dong and Mao (Requicha, 1999) have reported the synthesis and characterization of polystyrene nanorods. After 3 hours reaction time, they produced nanorods with length = 1 μm and width = 60–85 nm (Requicha, 1999).

Polystyrene nanoparticles are pushed on transparent glass slide (ITO glass) substrate using the Si AFM probe. This model is verified by using available theoretical and experimental results. Then polystyrene nanorod is pushed to study the process. In this simulations, polystyrene nanorod with diameter Rp=85 nm and different length are pushed on the ITO glass substrate that moves with 5nm/s constant velocity. Contact mechanics and tribological parameters can be obtained experimentally for different materials which are in contact (Table 3). The constant friction coefficients for static and dynamic movement of the nanoparticle on the substrate are μs=0.8, μd=0.7, respectively. Shear strength is assumed to be constant on the both contact surfaces between the particle/substrate and the tip/substrate. Surface energy between the nanorod and the tip/substrate is ω=0.1 J/m2 and contact angle is φ =45 (Israelachvili, 1991).

Geometrical parameters					Mechanical properties			
L(μm)	W(μm)	t(μm)	H(μm)	R_t(nm)	E(GPa)	υ	G(GPa)	ρ(kg/m^3
225	48	1	12	20	169	0.27	66.54	2330

Table 2. Geometrical and mechanical parameters of the AFM cantilever

Friction Coefficient		Shear Strength	
μ_s	μ_r (nm)	S_s (MPa)	S_r (Pa.m)
0.8	80	28	28

Table 3. Tribological parameters between nanorod/substrate (Israelachvili, 1991)

7. Results and discussions

As mentioned in Modeling based on AFM Section, the manipulation process modeling is presented considering various forces and nano-scale features. A polystyrene nanorod with 85 nm diameter and 1 μm length is selected to push on the ITO glass substrate.

Initially, the tip has 50 nm distances from the nanorod in both vertical and longitudinal directions. Since the stage moves with a constant velocity (5 nm/s), the probe moves down to reach 1.5 nm in heights (instability region) after 9.7 seconds (Fig. 11). In this region, the probe snaps in the substrate. Jump to the surface can be detected using registered photodiode data. Then, the cantilever moves up to overcome the adhesion forces. The probe motion will continue to reach 16 nm heights (pull out). Then, the cantilever moves up 73 nm after 11.4 seconds to create a proper contact angle. After that, it moves 90 nm after 9 seconds to contact with the desired nanorod, horizontally. The tip jumps to the particle when the

tip–particle distance reaches to 10 nm. The probe is in contact with the nanorod and the necessary conditions for pushing are provided (Moradi et al., 2011).

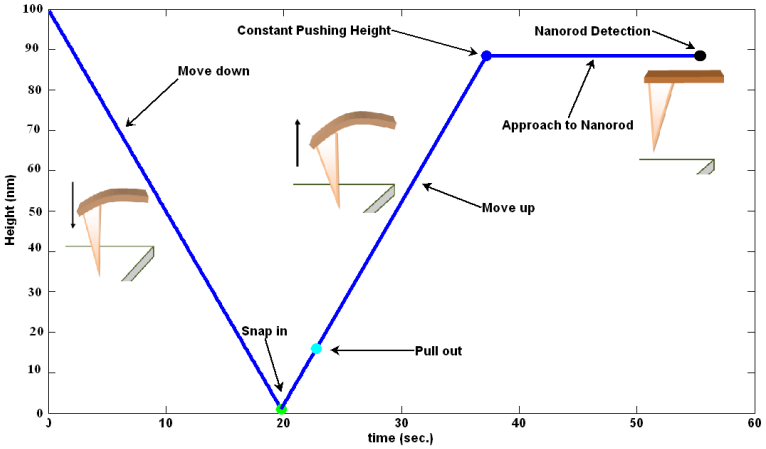

Fig. 11. Height & Time During approach/retract to the surface (Moradi et al., 2011)

The cantilever may pass over the nanorod and losses it during the pushing process. To prevent unpredicted effects and to ensure the desired contact angle of 45 degrees, initial offset in Z direction should be considered. Here 50 nm have been applied to the model. As shown in figure 12, initial pushing force is larger than critical sliding force on the tip. The substrate motion increases the pushing force to reach the critical sliding force. At critical time (0.17 seconds), the critical force (about 27.8 nN) overcomes the critical adhesion and friction forces (Table 4). The nanorod is stationary up to critical time. In the critical time, it begins sliding on the substrate. Unlike micro particles, for the nanorods, the sliding is dominant dynamic mode (Moradi et al., 2011).

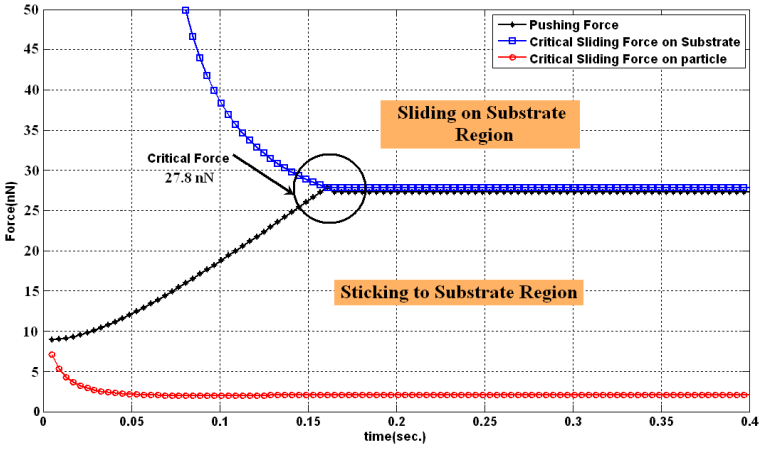

Fig. 12. Critical force to sliding the polystyrene nanorod on the ITO glass substrate (Moradi et al., 2011)

Here based on von mises yield criteria, particle damage condition is checked in each instance. Operation may be failed when safety factor being less than one. Shear force and moment variation along length are used to calculate safety factor in critical time. Using common elastic relations (Dong & Mao, 2005), the Safety factor for this process is estimated about 1.01 that shows safe pushing process of nanorod to a desired position. Complete nanorod pushing procedure consists of initial position, maximum deflection of the nanorod at critical time, the nanorod motion in each instance and the final desired position respectively (Fig. 13). This process takes about 50 seconds, totally (Moradi et al., 2010, 2011).

No	Process Output	Value
1	Critical Force (nN)	27.8
2	Critical Time (Sec.)	0.161
3	Maximum Deflection (nm)	75
4	Maximum Indention (nm)	0.033
5	Process Safety Factor	1.01
6	Adhesion Energy (10^{-16}J)	1.38
7	Potential Energy (10^{-16}J)	10.4

Table 4. Results of process simulation

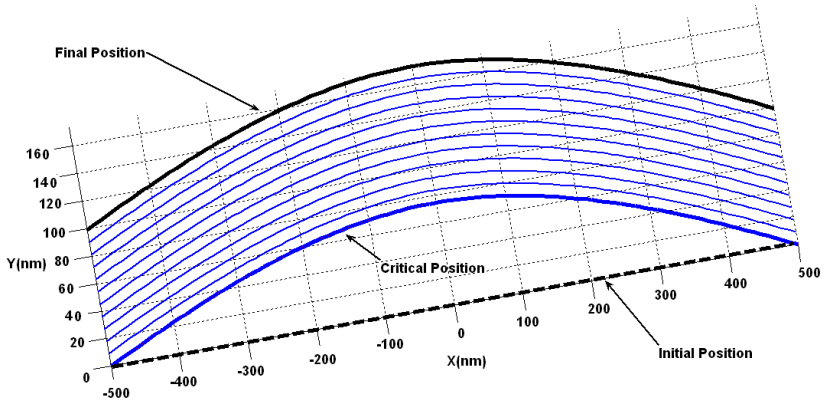

Fig. 13. The polystyrene nanorod pushing procedure to a desired position (Moradi et al., 2010, 2011)

7.1 After manipulation

When nanorod reached to desired position, tip move upward and goes to reference position. There is a question that based on adhesive force, if nanorod remain deflected or no. To answer this question, first we calculate adhesion energy using JKR theory (44) and potential energy (45) in deflected position. Then, these values are compared. Nanorod relaxes to its straight shape If adhesion energy is less than potential energy else it remain deflected. Figure (14) shows these energy values for different aspect ratio. As shown in this figure, when aspect ratio is less than 6, nanorod remain deflected after tip removal. But for higher aspect ratio, adhesion force can't keep it deflected. So, nanorod starts to relax to its straight position.

$$U_{adhesion} = 2\int_{-L/2}^{+L/2} (2\omega)b(x)dx \tag{44}$$

$$U_{Potential} = \int_{-L/2}^{+L/2} F_T x dx \tag{45}$$

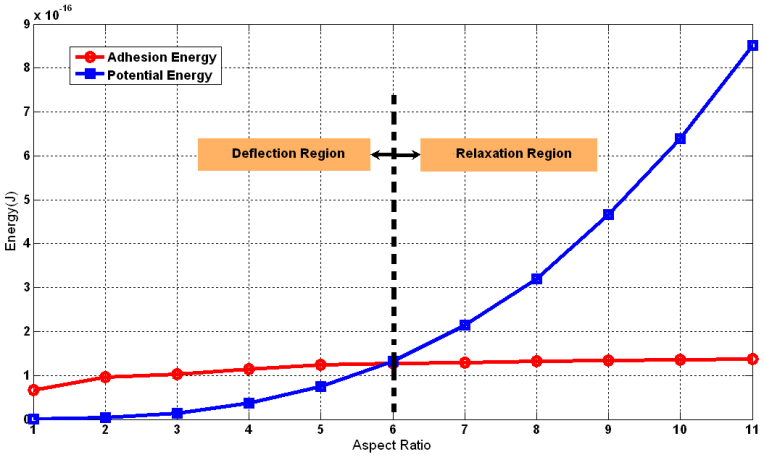

Fig. 14. Aspect ratio effects on adhesion and potential energy

7.2 Nanorod length effect analysis

The effect of aspect ratio on the process is one of the most important issues in manipulation of Nanorods. To study this parameter, a lot of simulations are repeated for different aspect ratio with constant radius. For aspect ratios 1:1 to 1:11, effects on the process are shown in Fig. 15. As shown in Fig. 15, for very short length (1:1 aspect ratio), deflection is very small

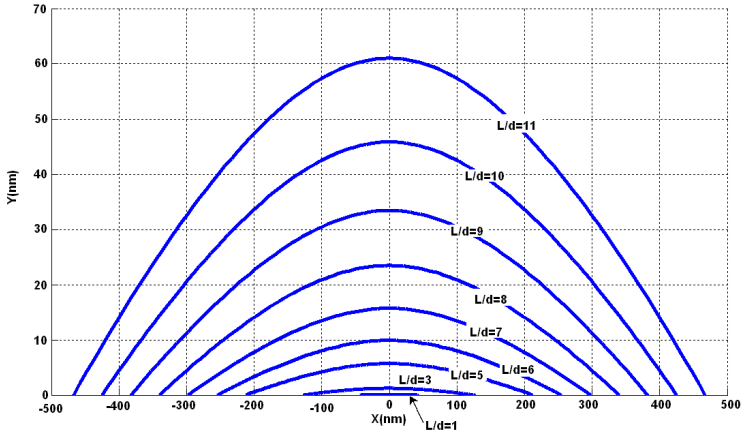

Fig. 15. Aspect ratio effects on deflection and motion of a nanorod (Moradi et al., 2010)

and negligible. The length increment causes the deflection to be more considerable. The maximum deflection is observed at 61 nm in 1:11 aspect ratios. The purpose of manipulation was 100 nm displacements in the straight path, but the longest nanorod pushed 61 nm because of the critical deflection. So, for fabrication in the nanoscale, deflection should be considered before process setting. To ensure a safe process, yield criteria, maximum shear and deflection should be considered. Using Von Mises theory, the safety factor is calculated for each one. When the aspect ratio is greater than 1:11.76, the nanorod approaches the failure region and may be damaged. Owing to the adhesion force, increasing the aspect ratio causes critical force and time increment, respectively (Moradi et al., 2010).

Also, based on presented model, for different aspect ratio pushing force and maximum deflection are obtained. As shown in figure 16, increase in aspect ratio increase these two outputs respectively.

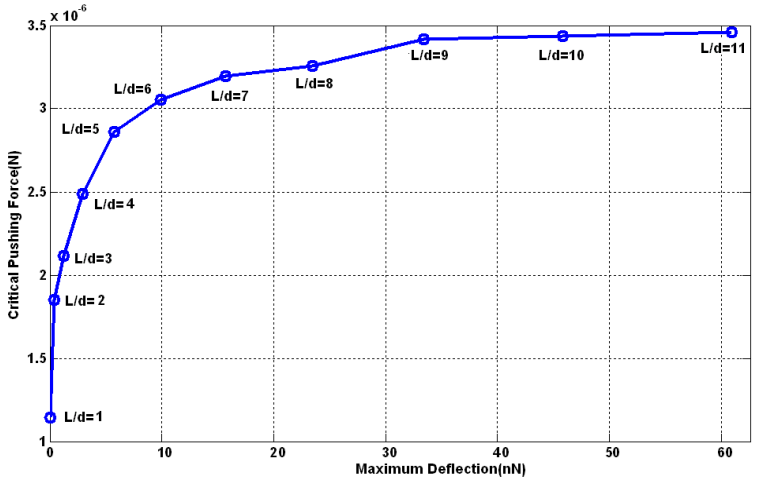

Fig. 16. Aspect ratio effects on Critical pushing force and maximum deflection

9. Conclusion

Using accurate model in the nano scale, physical phenomena of nanotechnology can be understood. However, this model can be used in accurate prediction of manipulation of Nanorods, control of process, optimization of parameters and user interface system development for SPMs. In addition, it can be a suitable tool in automation of nano assembly and nano manufacturing.

It obviously has been shown that after manipulation, nanorod relaxes to its straight shape If adhesion energy is less than potential energy else it remain deflected. When aspect ratio is less than 6, nanorod remain deflected after tip removal. But for higher aspect ratio, adhesion force can't keep it deflected. So, nanorod starts to relax to its straight position. In addition, in this book chapter, using Von Mises theory, the safety factor is calculated for various criterions. When the aspect ratio is greater than 1:11.76, the nanorod approaches the failure region and may be damaged. Owing to the adhesion force, increasing the aspect ratio causes critical force and time increment, respectively

Also, based on presented model, for different aspect ratio pushing force and maximum deflection are obtained. As shown in figures, increase in aspect ratio increase these two outputs respectively.

10. References

http://www.en.wikipedia.org/wiki/Nanorod

http://www.articleworld.org/index.php/Nanorod

K. Mølhave, T. Wich, A. Kortschack, "Bøggild, P. Pick-and-place nano-manipulation using microfabricated grippers", Nanotechnology 2006, 17, 2434-2441.

M. Sitti, "Survey of nano-manipulation systems", In Proc. IEEE Nanotechnology Conference, 2001, Maui, HI, 75–80.

Moradi M., Fereidon A. H., Sadeghzadeh S.,"Dynamic modeling for nano-manipulation of polystyrene nanorod by atomic force microscope", Scientia Iranica 2011, 18 (3), 808–815.

X. Tian et al., "A Study on Theoretical Nano Forces in AFM Based Nano-manipulation", Proc. of the 2nd IEEE Int. Conf. on Nano/Micro Engineered and Molecular Systems, 2007.

B. Bhushan, "Nanotribology and Nanomechanics: an introduction", 2005, Springer-Verlag.

J.N. Israelachvili, "*Intermolecular and surface forces*", 1991, Academic Press, London.

M. Sitti, H. Hashimoto, "Controlled Pushing Of Nanoparticles: Modeling And Experiments", Proc. of IEEE/ASME Trans. on Mechatronics, Vol. 5, No. 2, (2000).

J.M. Serafin, A.A. Gewirth, "Measurement of Adhesion Force to Determine Surface Composition in an Electrochemical Environment", J. Phys. Chem. B, 101, (1997) 10833-10838.

M.R. Falvo et al., "Nanometre-scale rolling and sliding of carbon nanotubes", Nature, 397 (1999) 236-8.

M.R. Falvo et al., "Manipulation of Individual Viruses: Friction and Mechanical Properties'', Biophysical J., Vol. 72, (1997) 1396-1403.

S. Wu et al., "Manipulation and behavior modeling of one-dimensional nanomaterials on a structured surface'', App. Surface Sci., (2010).

J.C. Hsu, R.P. Chang, W.J. Chang, ''Resonance Frequency of Chiral SWNT using Timoshenko Beam Theory'', Phys. Letters A, 372, (2008) 2757-2759.

A.P. Boresi, O.M. Sidebottom, F.B. Seely, J.O. Smith, "*Advanc*ed *Mechanics of Materials*", 1993, John Wiley and Sons.

A.G. Requicha, "*Nanorobotics: Handbook of Industrial Robotics*", 2nd ed., 1999, Wiley, pp 199–210.

A. Tafazzoli, M. Sitti, "Dynamic modes of nanoparticle motion during nano probe based manipulation", Proc. Of IMECE'04, 2004.

M.H. Korayem, M. Zakeri, "Sensitivity analysis of nanoparticles pushing critical conditions in 2-D controlled nano-manipulation based on AFM", Int. J. Adv. Manuf. Technol. , (2008).

A. Tafazzoli, C. Pawashe, M. Sitti, "Atomic force microscope based two-dimensional assembly of micro/ nanoparticles", (ISATP 2005) 6th IEEE Int. Symp., 230 – 235, 2005.

Moradi M., Fereidon A. H., Sadeghzadeh S., "Aspect Ratio and Dimension Effects on Nonorod Manipulation by Atomic Force Microscope (AFM)", Micro Nano Letters, 5, 5, 324–327, 2010.

J. Dong, G. Mao, "Polystyrene nanorod formation in $C_{12}E_5$ hemimicelle thin film templates", Colloid Polym. Sci. (2005) 284: 340–345.

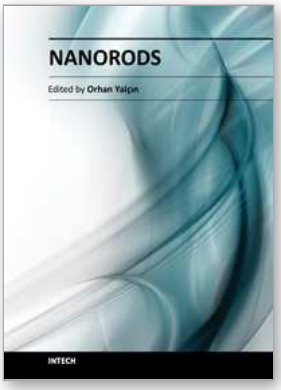

Nanorods

Edited by Dr. Orhan Yalçın

ISBN 978-953-51-0209-0
Hard cover, 250 pages
Publisher InTech
Published online 09, March, 2012
Published in print edition March, 2012

The book "Nanorods" is an overview of the fundamentals and applications of nanosciences and nanotechnologies. The methods described in this book are very powerful and have practical applications in the subjects of nanorods. The potential applications of nanorods are very attractive for bio-sensor, magneto-electronic, plasmonic state, nano-transistor, data storage media, etc. This book is of interest to both fundamental research such as the one conducted in Physics, Chemistry, Biology, Material Science, Medicine etc., and also to practicing scientists, students, researchers in applied material sciences and engineers.

How to reference

In order to correctly reference this scholarly work, feel free to copy and paste the following:

A. H. Fereidoon, M. Moradi and S. Sadeghzadeh (2012). Manipulation of Nanorods on Elastic Substrate, Modeling and Analysis, Nanorods, Dr. Orhan Yalçın (Ed.), ISBN: 978-953-51-0209-0, InTech, Available from: http://www.intechopen.com/books/nanorods/manipulation-of-nanorods-on-elastic-substrate-modeling-and-analysis

INTECH
open science | open minds

InTech Europe
University Campus STeP Ri
Slavka Krautzeka 83/A
51000 Rijeka, Croatia
Phone: +385 (51) 770 447
Fax: +385 (51) 686 166
www.intechopen.com

InTech China
Unit 405, Office Block, Hotel Equatorial Shanghai
No.65, Yan An Road (West), Shanghai, 200040, China
中国上海市延安西路65号上海国际贵都大饭店办公楼405单元
Phone: +86-21-62489820
Fax: +86-21-62489821